Available online at www.sciencedirect.com
ScienceDirect
Journal of Hazardous Materials 152 (2008) 397–406
Journal of Hazardous Materials
www.elsevier.com/locate/jhazmat

Simultaneous removal of perchlorate and arsenate by ion-exchange media modified with nanostructured iron (hydr)oxide

Kiril Hristovski [a,*], Paul Westerhoff [b,1], Teresia Möller [c,2], Paul Sylvester [c,2], Wendy Condit [d,3], Heath Mash [e,4]

[a] *Environmental Technology Laboratory, Arizona State University, 6075 S. WMS Campus Loop W, Mesa, AZ 85212, United States*
[b] *Department of Civil and Environmental Engineering, Arizona State University, Box 5306, Tempe, AZ 85287-5306, United States*
[c] *SolmeteX Inc., 50 Bearfoot Road, Northborough, MA 01532, United States*
[d] *Battelle, 505 King Avenue, Columbus, OH 43201, United States*
[e] *United States Environmental Protection Agency, 26W. Martin Luther King Dr., Cincinnati, OH 45268, United States*

Received 1 May 2007; received in revised form 2 July 2007; accepted 3 July 2007
Available online 10 July 2007

Abstract

Hybrid ion-exchange (HIX) media for simultaneous removal of arsenate and perchlorate were prepared by impregnation of non-crystalline iron (hydr)oxide nanoparticles onto strong base ion-exchange (IX) resins using two different chemical treatment techniques. In situ precipitation of Fe(III) (M treatment) resulted in the formation of sphere-like clusters of nanomaterials with diameters of ~5 nm, while $KMnO_4$/Fe(II) treatments yielded rod-like nanomaterials with diameters of 10–50 nm inside the pores of the media. The iron content of most HIX media was >10% of dry weight. The HIX media prepared via the M treatment method consistently exhibited greater arsenate adsorption capacity. The fitted Freundlich adsorption intensity parameters ($q = K \times C_E^{1/n}$) for arsenate ($1/n < 0.6$) indicated favorable adsorption trends. The K values ranged between 2.5 and 34.7 mgAs/g dry resin and were generally higher for the M treated media in comparison to the permanganate treated media. The separation factors for perchlorate over chloride ($\alpha_{Cl^-}^{ClO_4^-}$) for the HIX media were lower than its untreated counterparts. The HIX prepared via the M treatment, had higher $\alpha_{Cl^-}^{ClO_4^-}$ than the HIX obtained by the $KMnO_4$/Fe(II) treatments suggesting that permanganate may adversely impact the ion-exchange base media. Short bed adsorber (SBA) tests demonstrated that the mass transport kinetics for both ions are adequately rapid to permit simultaneous removal using HIX media in a fixed bed reactor.

Keywords: Arsenate; Perchlorate; Hybrid ion exchange; Iron (hydr)oxide; Removal; Water

1. Introduction

Water supplies potentially contain multiple pollutants, each of which may require different treatment approaches. Technologies that can simultaneously remove multiple pollutants need to be developed. Perchlorate and arsenate are two of the many emerging contaminants. In this research, iron nanomaterials commonly used for arsenic removal are impregnated into the pores of perchlorate selective ion-exchange (IX) media. The resulting adsorbent is termed a hybrid ion-exchange (HIX) media, which, in this case, is capable of simultaneously removing both arsenic and perchlorate.

In its use as a rocket fuel additive, perchlorate has been released into the environment during the fabrication and demilitarization of weaponry [1]. Perchlorate in groundwater has also been associated with natural sources [2–4]. Perchlorate exposure has been implicated in health problems, including thyroid hormone and neurodevelopment disruption [5,6]. In 2005, the United States Environmental Protection Agency (US EPA) established a reference dose of 0.0007 mg/kg/day, which translates into a Drinking Water Equivalent Level (DWEL) of 24.5 μg/L [7].

* Corresponding author. Tel.: +1 480 727 1132; fax: +1 480 727 1684.
E-mail addresses: kiril.hristovski@asu.edu (K. Hristovski), p.westerhoff@asu.edu (P. Westerhoff), tmoller@solmetex.com (T. Möller), psylvester@solmetex.com (P. Sylvester), conditw@battelle.org (W. Condit), mash.heath@epa.gov (H. Mash).
[1] Tel.: +1 480 965 2885; fax: +1 480 965 0557.
[2] Tel.: +1 508 393 5115; fax: +1 508 393 1795.
[3] Tel.: +1 614 424 3501; fax: +1 614 458 3501.
[4] Tel.: +1 513 569 7713; fax: +1 513 487 2543.

0304-3894/$ – see front matter © 2007 Elsevier B.V. All rights reserved.
doi:10.1016/j.jhazmat.2007.07.016

Table 1
Commercial perchlorate specific IX media used in the study

Media Name	Manufacturer	Functional groups	ClO_4^- selectivity	Exchange capacity (meq/mL)	D_P (mm) (mesh-size) as reported
Amberlite PWA2	Rohm&Haas	NA	High	0.6	0.3–1.2 (16–50)
A-530E	Purolite	$(Ethyl)_3N/(hexyl)_3N$	High	0.55	(16–50)
SIR-110	ResinTech	$(Butyl)_3N$	High	0.6	0.3–1.2 (16–50)
CalRes 2103	Calgon	Quaternary amine	High	1.4 (max)	(16–50)
A-520E	Purolite	$(Ethyl)_3N$	Moderate	0.9	0.3–1.2 (16–50)
SIR-100	ResinTech	$(Ethyl)_3N$	Moderate	0.85	0.3–1.2 (16–50)

The International Agency for Research on Cancer classifies arsenic as a Class A human carcinogen [8]. Many community water systems and private wells in North America and around the world contain arsenic concentrations exceeding the maximum contaminant level (MCL) of 10 μg/L promulgated by the US EPA, European Union (EU) and World Health Organization (WHO) [9–14].

Concentrations of arsenate and perchlorate can be high enough to require removal of both before water can be used for drinking. Several commercially available technologies can remove either arsenic or perchlorate from drinking water. Because perchlorate is considered a non-coordinating ligand, existing removal technologies generally utilize strong base ion-exchange media. These have been applied to simultaneous removal of heavy metals such as uranium [15–17]. In contrast, arsenic adsorbs onto metal (hydr)oxide surfaces by forming inner-sphere bidentate ligands [18,19]. Although anion-exchange resins and iron flocculation processes have been used in arsenic removal, many removal technologies focus on metal (hydr)oxides as adsorbent media. These include granular iron (hydr)oxides, activated alumina, titanium, and other (hydr)oxides [20–24].

Metal (hydr)oxides have been combined with support materials such as granulated activated carbon (GAC) or polymeric resin to fabricate adsorbent media capable of simultaneous removal of multiple contaminants [25–29]. Cumbal and Sengupta [30] studied the effect of positively and negatively charged groups on the arsenic adsorption, also known as the Donnan exclusion effect. Their work demonstrates that hybrid ion-exchange media capable of simultaneous removal of arsenate and perchlorate can be developed by precipitating hydrous ferric oxide nanoparticles onto perchlorate selective ion-exchange (IX) media. Although Cumbal and Sengupta [30] showed that their HIX media can simultaneously remove perchlorate and arsenate in a fixed bed column, their work did not investigate different iron precipitation processes or their impact on the performance of the HIX media. Crosby et al. [31] found that ferric (hydr)oxide nanoparticles prepared in aqueous environments can have spherical or rod-like shapes depending on whether they are derived from Fe^{2+} or Fe^{3+} ions. Therefore, the goal of this study was to explore (1) whether spherical and rod-like shaped nanoparticles can be precipitated onto strong base IX media using approaches similar to those demonstrated by Crosby et al. [31] and (2) whether the newly prepared hybrid ion-exchange media can simultaneously remove arsenate and perchlorate from simulated groundwater in a packed short bed column.

To achieve this goal, the following tasks were carried out: (1) six commercially available macroporous strong base IX (polystyrene crosslinked with divinylbenzene) media capable of removing perchlorate were impregnated with ferric (hydr)oxide nanoparticles using different chemical treatments; (2) HIX media were characterized by elemental analysis, powder X-ray diffraction (XRD), and focused ion beam/scanning electron (FIB/SEM) and light microscopy techniques; (3) equilibrium tests were performed in bicarbonate buffered distilled water; (4) for arsenate and perchlorate, Freundlich adsorption isotherm parameters and separation factors, respectively, were estimated; (5) continuous flow tests in model groundwater were conducted to confirm that the HIX media exhibits mass transfer properties that enable it to simultaneously remove arsenate and perchlorate in a column setup.

2. Experimental approach

2.1. Preparation of hybrid ion-exchange media

Six commercially available, perchlorate selective ion-exchange resins (Table 1) were impregnated with iron (hydr)oxide using two different chemical treatment techniques. In the first technique $KMnO_4$ oxidizes Fe(II) in situ, and ferric (hydr)oxide nanoparticles subsequently precipitate [32]. In the second method Fe(III) precipitates as iron (hydr)oxide nanoparticles under alkaline conditions.

Three different chemical formulations were used to prepare HIX via the $KMnO_4$/Fe(II) treatment process. These are identified as L, H, and K. In general, 67 g of resin was vigorously stirred in 800 mL of $KMnO_4$ solution with concentrations presented in Table 2. The resin was rinsed with distilled water to remove excess MnO_4^- and reacted with 800 mL of $FeSO_4{\cdot}7H_2O$ for 6 h to oxidize the Fe(II). This reaction is illustrated in Eq. (1):

$$8H_2O + 5Fe^{2+} + MnO_4^- \rightarrow 5FeOOH_{(s)} + 7H^+ + Mn^{2+} \quad (1)$$

Table 2
Reagent concentrations and contact times for the $KMnO_4$/Fe(II) preparation process

Treatment code	$KMnO_4$ (g/L)	$FeSO_4{\cdot}7H_2O$ (g/L)	Contact time (min)
L	12.6	111.3	15
K	12.6	111.3	45
H	25.2	166.9	15

Table 2 presents $KMnO_4$ and $FeSO_4{\cdot}7H_2O$ concentrations and contact times for each formulation.

According to Eq. (1), Fe(II) oxidation by permanganate generates H^+ and thus decreases the pH. To remove excess protons and iron (hydr)oxide precipitate, the product was rinsed and soaked overnight in a solution of 1% $NaHCO_3$ and in distilled water, and stored wet. The formula $FeOOH_{(s)}$ expresses the formation of an amorphous ferric (hydr)oxide precipitate.

A proprietary synthetic method, developed by SolmeteX, using a solution of $FeCl_3$ in alcohol was used to synthesize HIX by precipitation of Fe(III) as iron (hydr)oxide under alkaline conditions (M treatment). For 1 h, 50 mL of IX resin was vigorously stirred with 200 mL of $FeCl_3$ solution. The iron-impregnated resin was filtered under suction and dried at room temperature. The dried resin was then vigorously stirred with a NaOH solution for 30 min to form a precipitate. The product was rinsed with distilled water to lower the pH and remove excess precipitate. The entire process was repeated for another contact cycle, after which the product was repeatedly rinsed and soaked in 5% NaCl solution until pH < 8 in order to convert the resin back to its chloride form. The product was repeatedly rinsed with distilled water to remove excess NaCl and stored wet. Eq. (2) illustrates the precipitation of iron via this second technique:

$$Fe^{3+} + 3OH^- \rightarrow FeOOH_{(s)} + H_2O \quad (2)$$

2.2. Characterization of HIX

The iron content of HIX was quantitatively determined by acid digestion of the dry HIX resin in concentrated HNO_3 and 30% H_2O_2 (US EPA SWA 846, Method 3050B) followed by Flame-Atomic Absorption Spectroscopy analysis (Smith-Hieftje 12, Instrumentation Laboratory Inc.) [33]. Before the acid digestion, the HIX was dried at 104 °C to constant mass to remove any moisture. The repetitive addition of 30% H_2O_2 to the sample aliquot during digestion resulted in disintegration of the polymeric base of the media and complete release of the iron into the solution. Light microscopy was used to qualitatively determine the distribution of iron (hydr)oxide in the resins. Focus ion beam and scanning electron microscope techniques were employed to determine the size and the shape of the deposited iron (hydr)oxide nanoparticles within the pores of the media (Nova 200 NanoLab UHR FEG-SEM/FIB). The structure and type of the iron (hydr)oxide was evaluated using X-ray diffraction (Bruker SMART APEX).

2.3. Equilibrium adsorption experiments

Arsenate equilibrium adsorption experiments with no perchlorate present were conducted at a target pH 7.5 ± 0.25 (final pH) in the presence of 5 mM $NaHCO_3$ and 9.15×10^3 μg/L As(V). Equilibrium experiments with only perchlorate in solution were also conducted at a target pH 7.5 ± 0.25 (final pH) in the presence of 10 mM $NaHCO_3$ and 7.90×10^3 μg/L ClO_4^-. Experiments were conducted in 50 mL centrifuge vials with HIX adsorbent dosages of 5–300 mg dry resin (five data points were considered for each isotherm). Samples were continuously agitated for 3 days prior to separating the resin by gravity settling. Isotherms were developed for arsenate adsorption and analyzed using the Freundlich adsorption isotherm model (Eq. (3).

$$q = K \times C_E^{1/n} \quad (3)$$

where q is adsorption capacity (mg adsorbate/g adsorbent), K the Freundlich adsorption capacity parameter ((mg adsorbate /g adsorbent) × (L/mg adsorbate)$^{1/n}$), C_E the equilibrium concentration of adsorbate in solution (mg adsorbate/L), and $1/n$ is the Freundlich adsorption intensity parameter (unitless).

The perchlorate removal by the hybrid ion-exchange media was evaluated by estimating the separation factors of the media for perchlorate over chloride, $\alpha_{Cl^-}^{ClO_4^-}$. Since the systems were characterized by ternary ion exchange (perchlorate, chloride and bicarbonate), which is more difficult to describe, several assumptions were made to simplify the system.

According to Crittenden et al. [34], the approximate separation factor for perchlorate over bicarbonate is $\alpha_{HCO_3^-}^{ClO_4^-} > 500$ for strong base anion resins with polystyrene divinylbenzene matrix and tertiary amine functional groups in solutions with TDS = 250–500 mg/L as $CaCO_3$ (0.005–0.010N solutions). As such, it can be assumed that bicarbonate would not cause interference with the perchlorate/chloride ion exchange, and the system can be simplified and evaluated as binary ion exchange (perchlorate and chloride), which is easier to describe. It was also assumed that there is not excess Cl^- remaining inside the pores of the HIX media as a result of the synthesis process, and that the only excess Cl^- was the one resulting from the addition of HCl used for pH correction. Using MINEQL+, the excess chloride was estimated to be $C_{E\text{-}Cl} \approx 3 \times 10^{-4}$ M for pH 7.7 in 10 mM bicarbonate buffered nanopure water [35].

The binary separation factor α_j^i is a measure of the preference for one ion over another during ion exchange and can be expressed using Eq. (4) [34]:

$$\alpha_j^i = \frac{Y_i \times X_j}{Y_j \times X_i} \quad (4)$$

where X_j is the equivalent fraction of presaturation ion in aqueous phase, X_i the equivalent fraction of counterion in aqueous phase, Y_j the resin-phase equivalent fraction of presaturation ion and Y_i is the resin-phase equivalent fraction of counterion.

The equivalent fraction in the aqueous phase is a ratio between the concentration of the ion in aqueous phase, $C_{i\text{ or }j}$ (eq/L) and the total aqueous concentration of the ion, C_T (eq/L) [34]:

$$X_i = \frac{C_i}{C_T}; \qquad X_j = \frac{C_j}{C_T} \quad (5)$$

The resin-phase equivalent fraction is a ratio between the resin-phase concentration of the ion, $q_{i\text{ or }j}$ (eq/L) and the total ion-exchange capacity of the resin, q_T (eq/L) [34]:

$$Y_i = \frac{q_i}{q_T}; \qquad Y_j = \frac{q_j}{q_T} \quad (6)$$

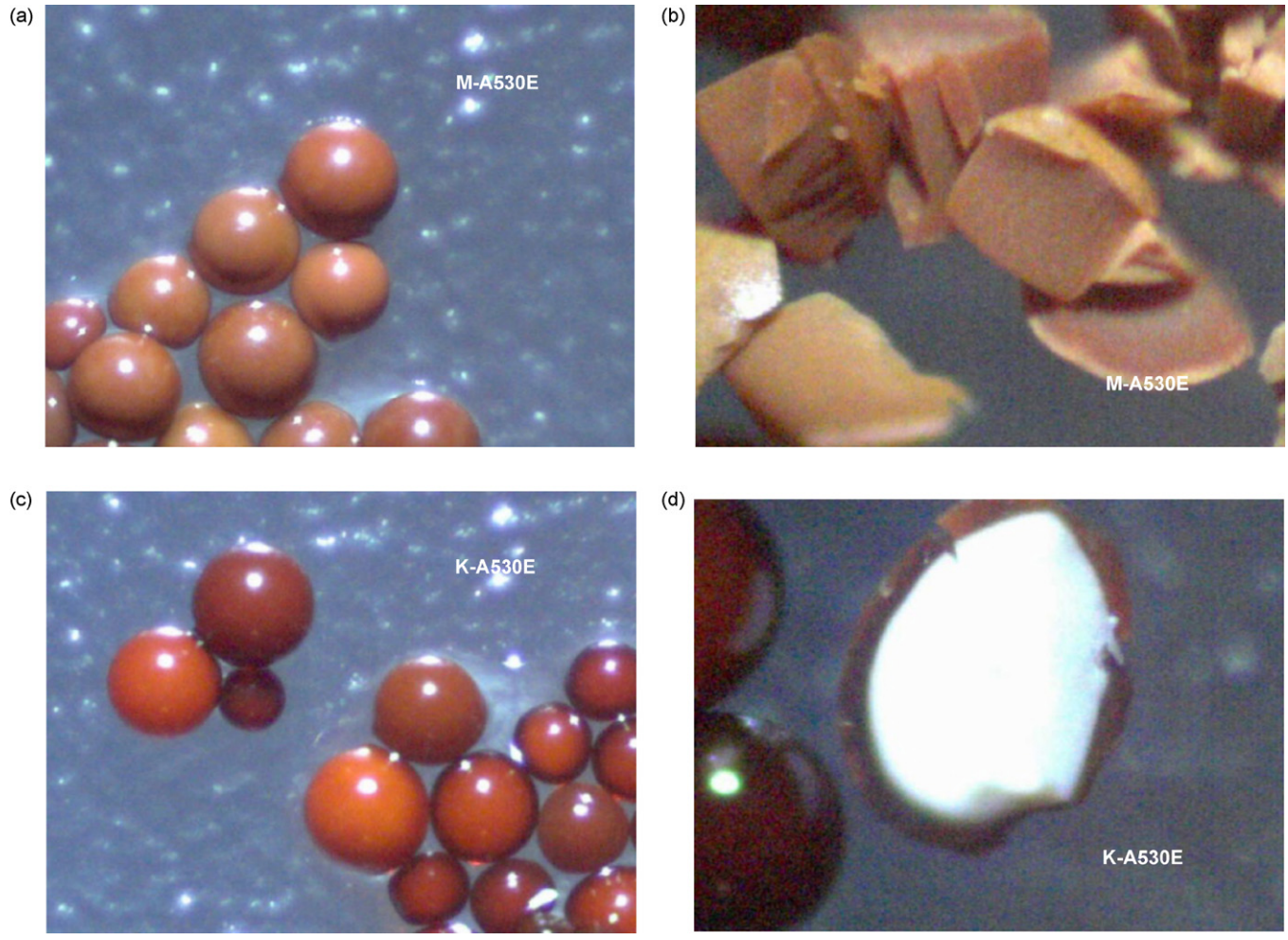

Fig. 1. Photographs of uncrushed and crushed M-A530E and K-A530E media obtained at 60× (a and c) and 200× (b and d) magnifications.

2.4. Dynamic fixed bed column tests

Short bed adsorber (SBA) tests were conducted on the HIX and virgin IX media with the highest adsorption capacities [36–39]. To assay whether the media would perform well when used in waters found in the environment, all SBA tests were conducted using modified NSF 53 Challenge water. The following target parameters describe the water chemistry of NSF 53 Challenge water: $[Mg^{2+}] = 12$ mg/L; $[SO_4{}^{2-}] = 50$ mg/L; $[N\text{-}NO_3{}^{-}] = 2$ mg/L; $[F^{-}] = 1$ mg/L; $[SiO_2] = 20$ mg/L; $[PO_4{}^{3-}] = 0.04$ mg/L; $[Ca^{2+}] = 40$ mg/L; $T = 20 \pm 2\,^{\circ}C$; turbidity < 1 NTU; and pH 7.5 ± 0.25. The water chemistry of NSF 53 Challenge water was modified by addition of $[As(V)] = 100$ μg/L and $[ClO_4{}^{-}] = 100$ μg/L as Na_2HAsO_4 and $KClO_4$.

The media was packed in a glass column atop a support of quartz sand. Glass beads were placed above and below the media to provide evenly distributed flow. The mass of the media was $\sim 0.6 \pm 0.1$ g. In the tests, the ratio of the column to particle diameter ranged from 9.2 to 36.7 due to the broad particle size distribution (300–1200 μm; geometric mean of 600 μm) of the virgin IX material used in fabrication. Media to inside column diameter ratios >8 are sufficiently large that the wall effect on mass transfer can be neglected [40].

2.5. Arsenate and perchlorate analysis

Arsenate was analyzed using a graphite furnace atomic absorption spectrophotometer (GF-AAS) Varian Zeeman Spectra 400, and the perchlorate was analyzed using an ion chromatograph Dionex LC20, with a CD20 conductivity detector, GP40 gradient pump and AS40 autosampler [41]. Dionex AS11 analytical column and AG11 guard column at ambient temperature were used in the analysis. Solution of 20% methanol/80% sodium hydroxide at a flow rate of 1 mL/min was used as eluent.

3. Results and discussion

3.1. Characterization of HIX media

The iron content of the fabricated HIX varied from 2 to 27% by dry resin weight, with most containing 15–25% (Table 3). The iron content of the virgin IX media was <0.005%, except A-530E and PWA2 media, which contained 0.007 and 0.04% by dry resin weight, respectively.

All media were photographed under light microscopy with 60× and 200× magnification. Images were taken of both whole and crushed media (e.g., Fig. 1 for M-A530 and K-A530). All

Table 3
Iron content after acid digestion of virgin IX and HIX media (percentage Fe per dry weight)

Base media	Chemical treatment methods				Virgin IX
	M	L	H	K	
SIR-100	23%	18%	19%	13%	<0.005%
SIR-110	16%	12%	14%	11%	<0.005%
A520E	24%	19%	23%	23%	<0.005%
A530E	20%	17%	24%	20%	0.007%
CalRes2103	23%	25%	27%	23%	<0.005%
PWA2	16%	11%	12%	1.7%	0.04%

HIX resins had an orange-brown external color, which indicates iron (hydr)oxides. Roughly 25% of the HIX resins exhibited a consistent reddish color, suggesting good distribution of iron throughout the resin. Other HIX resins were white at their cores, the same color as most virgin media, suggesting poor iron penetration. The HIX resins obtained via M treatment, appeared to have the most consistent penetration of iron to the center of the beads (Fig. 1b). Resins treated with the L, H and K processes contained iron deposits concentrated in their outer layers; little or no deposition had occurred toward the center of the beads (Fig. 1d).

FIB/SEM analysis of the HIX media confirmed the presence of nanoparticles in their pores. The backscatter detector used during the FIB/SEM analysis differentiated between heavier elements such as iron (white areas in Fig. 2) and lighter elements such as carbon, nitrogen, oxygen and hydrogen (darker areas in Fig. 2). As seen in Fig. 2a, the M process formed clusters of sphere-like nanoparticles each approximately 5 nm in diameter. $KMnO_4$/Fe(II) based treatments formed rod-like nanoparticles within the pores with diameters of 10–50 nm and lengths of 50–100 nm that were not uniformly distributed throughout the

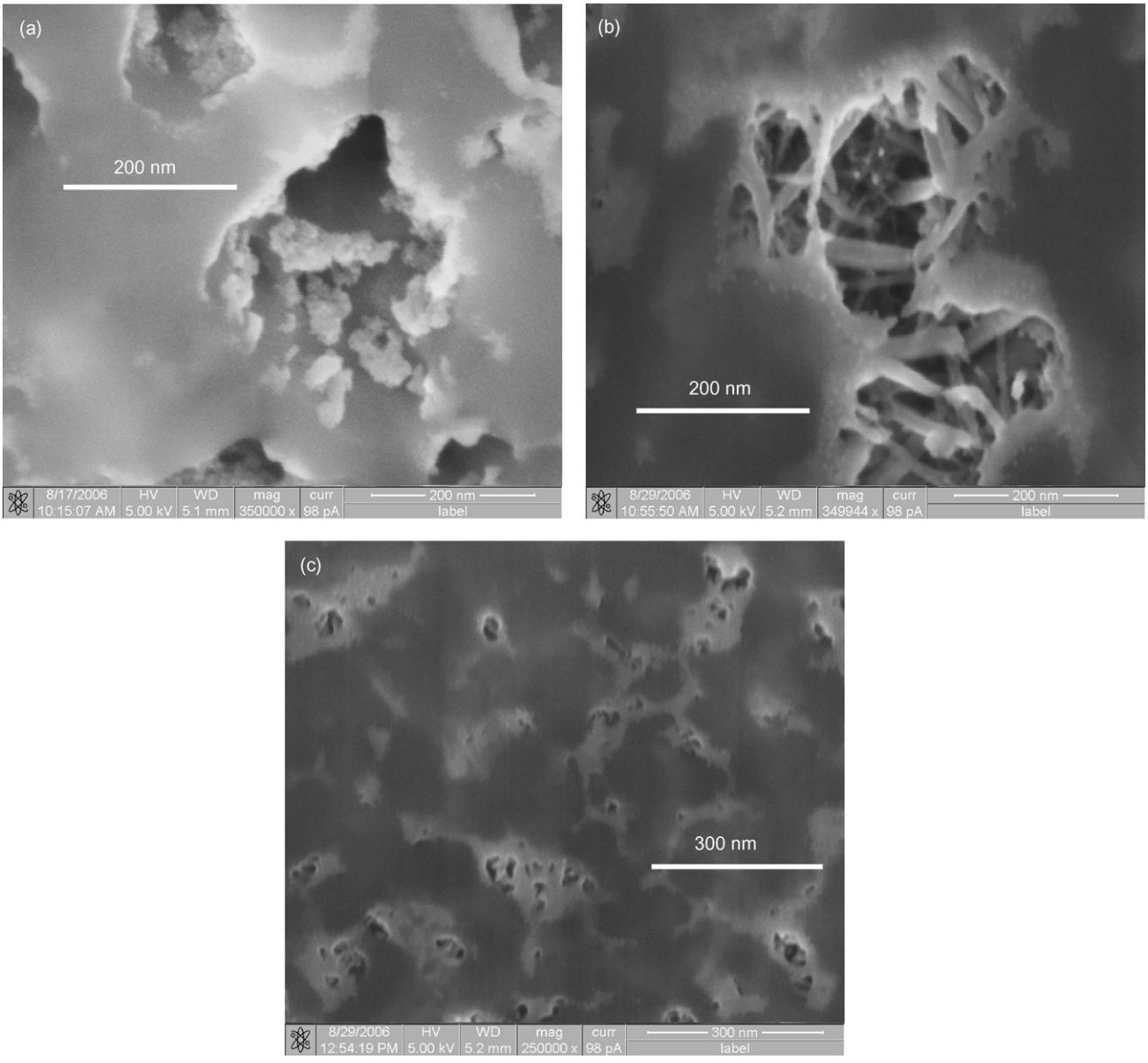

Fig. 2. FIB/SEM of MSEM of (a) M-CalRes (b) H-A530E, and (c) K-A530E. White areas indicate presence of iron; darker areas are the ion-exchange media material.

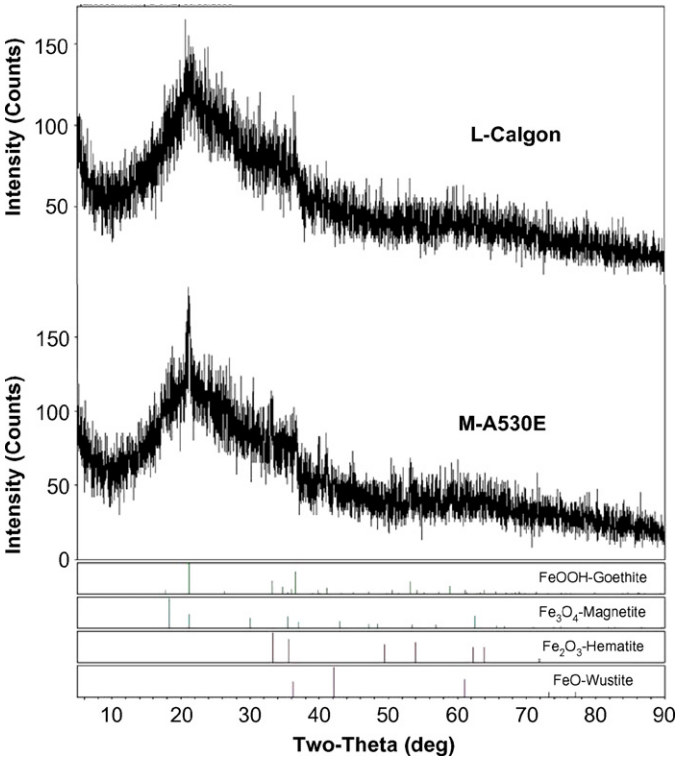

Fig. 3. X-ray diffraction spectra for the iron (hydr)oxide obtained from L-CalRes and M-A530.

resins (Fig. 2b). The FIB/SEM analysis also suggested that the nanoparticles precipitated by the $KMnO_4$/Fe(II) treatments can clog HIX media pores, as seen in Fig. 2c for L-A530E. Conversely, the nanoparticles obtained via M treatment method were more evenly distributed.

Powder XRD analysis suggested that all treatment processes yielded non-crystalline iron (hydr)oxide nanoparticles. The X-ray patterns for the ferric (hydr)oxides obtained via the M and $KMnO_4$/Fe(II) treatments exhibited peaks with the same two-theta degrees and intensities, implying that the treatment process did not influence the structure of the ferric (hydr)oxides. X-ray patterns for L-CalRes and M-A530E are shown in Fig. 3. These patterns were also exhibited by the other HIX media.

3.2. Equilibrium adsorption experiments

Fig. 4a presents the adsorption isotherms for arsenate for virgin CalRes 2103 media and the correspondent HIX media. The virgin IX media removed significantly less As(V) than did the HIX media (Fig. 4). For any given HIX resin, As(V) removal was generally quite uniform irrespective of the synthesis approach. Table 4 summarizes the Freundlich isotherm parameters for HIX and IX media. Adsorption is favorable when the adsorption intensity parameter ($1/n$) is <1. All fabricated HIX media had fitted values of $1/n < 0.5$ for arsenate except for H-A520 with $1/n = 0.6$. HIX prepared via the M treatment method had fitted arsenate adsorption capacity parameters (K_{As}) between 5.9 and 34.7 (mgAs/g dry resin)(L/mgAs)$^{1/n}$, while the $KMnO_4$/Fe(II) treatments yielded HIX media with K values between 2.5 and 22.4 (mgAs/g dry resin)(L/mgAs)$^{1/n}$. In general, M-prepared HIX media had slightly higher arsenate K_{As} values, suggesting better arsenate adsorption. In contrast to the HIX media, the virgin media exhibited higher $1/n$ values ($1/n > 1$) and lower K_{As} values ($K_{As} < 1.35$ ((mgAs/g dry resin)(L/mgAs)$^{1/n}$) for arsenate adsorption (except for $K_{As(V\text{-}100)} < 2.63$ ((mgAs/g dry resin)(L/mgAs)$^{1/n}$). This is to be expected since the iron (hydr)oxide adsorbs the arsenate. Relatively comparable values for K_{As} and $1/n$ are reported in the literature for granulated ferric hydroxide (GFH), which is one of the most commonly used adsorbents for arsenate treatment. Sperlich et al. [42] and Badruzzaman et al. [21] reported K_{As} values ranging between 30.8 and 74.2 ((mgAs/g GFH)(L/mgAs)$^{1/n}$), and $1/n$ values ranging between 0.16 and 0.36 for DI water at pH 7. These values are not much different from the ones estimated for the HIX if they are to be compared on basis of iron content, instead on basis of dry media mass.

To evaluate the effect of iron content on arsenate adsorption capacity, this capacity was calculated for each HIX media at equilibrium concentration $C_E = 100$ μg/L (i.e., ~99% arsenate removal). This was plotted against the media's iron content, as Fig. 4b illustrates. Although the figure shows no obvious trends, a liberal description of the data distribution suggests that the adsorption capacity initially increases as the iron content

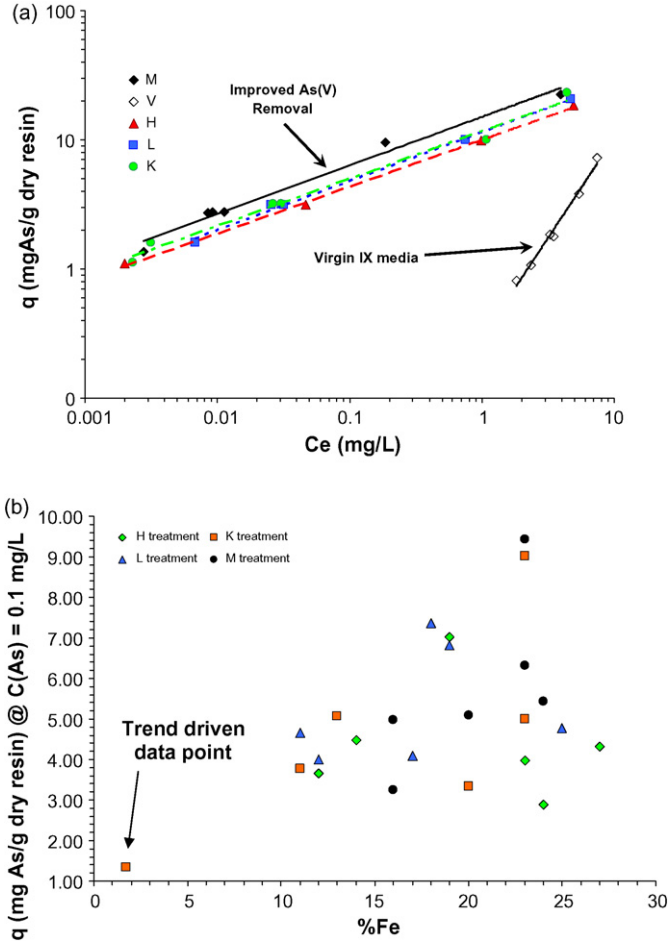

Fig. 4. Single solute adsorption isotherms for virgin and treated (a) Calgon CalRes 2103 media and (b) Resintech SIR-110 in $NaHCO_3$ buffered nanopure water. $pH_{Final} \approx 7.7$.

Table 4
Summary of Freundlich isotherm parameters (K and $1/n$) for arsenate and separation factors for perchlorate over chloride ($\alpha_{Cl^-}^{ClO_4^-}$) for HIX and virgin IX media

Media type	For As(V) adsorption (5 mM $NaHCO_3$ buffered nanopure water)			For ClO_4^- ion-exchange (10 mM $NaHCO_3$ buffered nanopure water)	
	K ((mg As/g dryresin)/(mg As/L))$^{1/n}$	$1/n$	R^2	$\alpha_{Cl^-}^{ClO_4^-}$ (mean value)	95% confidence limits
H-100	17.23	0.39	0.88	13.41	3.91
H-110	8.69	0.29	0.99	37.58	14.20
H-A520E	16.04	0.60	0.98	8.26	2.20
H-A530E	6.05	0.32	0.98	12.17	8.51
H-CalRes	9.94	0.36	1.00	5.23	2.92
H-PWA2	5.62	0.19	0.85	122.46	53.47
K-100	10.17	0.30	0.96	15.89	4.27
K-110	7.68	0.31	0.99	40.27	13.26
K-A520E	22.41	0.40	0.94	17.03	4.18
K-A530E	7.97	0.38	1.00	27.27	11.14
K-CalRes	11.63	0.37	0.99	10.39	4.93
K-PWA2	2.53	0.28	0.80	70.52	27.33
L-100	15.36	0.32	0.94	19.73	5.29
L-110	6.74	0.23	0.95	60.60	18.04
L-A520E	15.08	0.34	0.99	17.41	4.88
L-A530E	6.47	0.20	0.90	47.42	21.92
L-CalRes	11.40	0.38	1.00	7.51	3.51
L-PWA2	7.90	0.23	0.90	131.49	33.88
M-100	34.70	0.57	0.98	33.01	8.78
M-110	5.89	0.26	0.85	112.74	66.53
M-A520E	13.75	0.40	0.95	27.13	4.33
M-A530E	10.32	0.31	0.96	109.74	39.30
M-CalRes	15.03	0.38	0.98	30.43	13.85
M-PWA2	9.37	0.28	0.92	137.53	28.84
V-100	2.63	0.94	0.97	48.13	8.71
V-110	1.35	0.35	0.71	139.72	52.41
V-A520E	0.42	1.45	1.00	49.35	9.72
V-A530E	1.11	1.00	0.98	189.60	98.15
V-CalRes	0.29	1.55	0.99	45.92	22.65
V-PWA2	0.59	1.23	0.62	174.64	60.43

pH 7.75 ± 0.39.

increases until reaching a maximum capacity. After reaching the maximum, the adsorption capacity tends to decrease with increasing iron content due to probable pore clogging, as Fig. 2c illustrates. However, it must be noted that the discussed trend is strongly driven by a single data point at low Fe content. With exclusion of the trend driving data point, it appears that no obvious trends are present.

Table 4 also summarizes the calculated values for the separation factors ($\alpha_{Cl^-}^{ClO_4^-}$) for all media. The virgin IX media was characterized with highest separation factors for perchlorate in relation to its HIX counterparts. M types of media exhibited lower separation factors than its virgin counterpart IX media, which was probably due to blocking of the polymer ion-exchange sites by the iron (hydr)oxide nanoparticles. In contrast, the separation factors for M type HIX were higher than any of the permanganate treated counterpart media. This could be a result of two factors: (1) the blocking of ion-exchange sites by iron (hydr)oxide nanoparticles; and (2) oxidation of the polymer ion-exchange material by the permanganate. As illustrated in Fig. 5 for SIR-110 and PWA2 (both characterized with 16% Fe content), the M treatment yielded smaller decrease of the separation factor for SIR, than for PWA2. This suggests a possibility that the pore size distribution of the corresponding virgin IX media may be one of the factors influencing the magnitude of the blocking effect caused by the presence of iron (hydr)oxide nanoparticles.

Although it was not a focus of the study to evaluate the oxidizing impact of permanganate on the IX media, data anal-

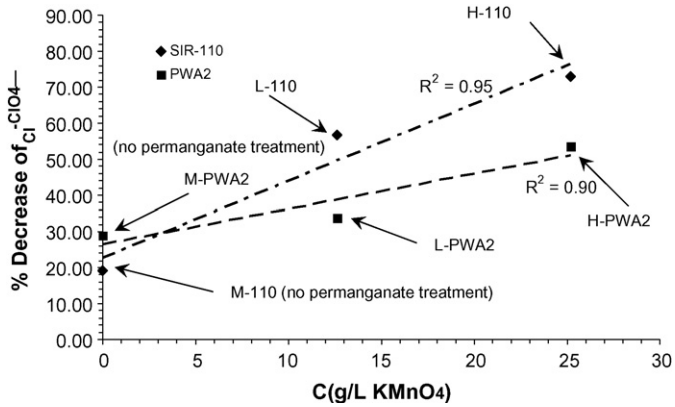

Fig. 5. Effect of $KMnO_4$ concentration on $\alpha_{Cl^-}^{ClO_4^-}$ for SIR-110 and PWA2. Contact time = 15 min.

ysis revealed a general trend exhibited in all media types. As illustrated in Fig. 5 for SIR-110 and PWA2 type media, the separation factor of the media decreases as permanganate concentration increases suggesting oxidation of the polymer ion-exchange material. This trend was typical for all HIX media fabricated from same IX media type. Since concentration of reacted permanganate was not measured and the extent of polymer oxidation is media specific, mass balances to quantify this process were not conducted.

3.3. Dynamic fixed bed column tests

A ranking methodology was used to select media for dynamic fixed bed column tests. First, adsorption capacities for arsenate (q, mg As/g dry resin) were calculated for C_E values of 0.1 mg/L (i.e., ~99% arsenate removal) based on the fitted Freundlich isotherm model parameters. Second, each HIX received an arsenate numerical score for a given C_E. The total number of HIX media was 24, so the HIX with the lowest q value received a score of 1, the next lowest received a 2, and so on to a value of 24 for the media with the highest q. Third, each HIX received a perchlorate numerical score based on the magnitude of its $\alpha_{Cl^-}^{ClO_4^-}$. Media with lowest $\alpha_{Cl^-}^{ClO_4^-}$ received a score of 1, and media with highest $\alpha_{Cl^-}^{ClO_4^-}$ received score of 24. The arsenate and perchlorate scores were added together to obtain the cumulative score. The highest of these indicated the HIX likely to be the best choice for both arsenate and perchlorate removal. From the media type with the highest cumulative ranking score, two HIX obtained via the two different treatments were selected as media for the dynamic packed bed column tests. PWA based HIX exhibited the highest score across both treatments. Thus L-PWA2, which had a higher overall ranking than H-PWA2 and K-PWA2, and M-PWA2 were selected together with their virgin counterpart.

An SBA column is a packed bed column with a bed of sufficiently short length that immediate concentration breakthrough occurs [43]. SBAs use full-size media in 2 cm packed columns and operate at the same loading rates as full-scale systems. Whereas the batch adsorption tests verified that arsenic and perchlorate could be removed when left to equilibrate for days, the SBA tests verified that the mass transfer kinetics of both arsenate and perchlorate were adequately rapid to permit simultaneous removal using HIX in a packed bed reactor.

Fig. 6 presents the results of the dynamic column tests for M-PWA2, L-PWA2 and V-PWA2 media. After 100 bed volumes of operation, the column effluent contains detectable levels of both arsenate and perchlorate. This is expected because the 2 cm media bed will not contain the entire mass transfer zone. The initial breakthrough value (C/C_0) is a function of the external mass transfer, which is a function of the flow velocity, media size and shape, and diffusivity of the solute. The D_l values for arsenate and perchlorate for single electrolyte solution at an infinite dilution are 9.05×10^{-6} and 1.79×10^{-5} cm^2/s, respectively, suggesting faster external mass transport for perchlorate [44]. Considering these D_l values, the external mass transfer coefficients (k_f) for arsenate and perchlorate were estimated using the

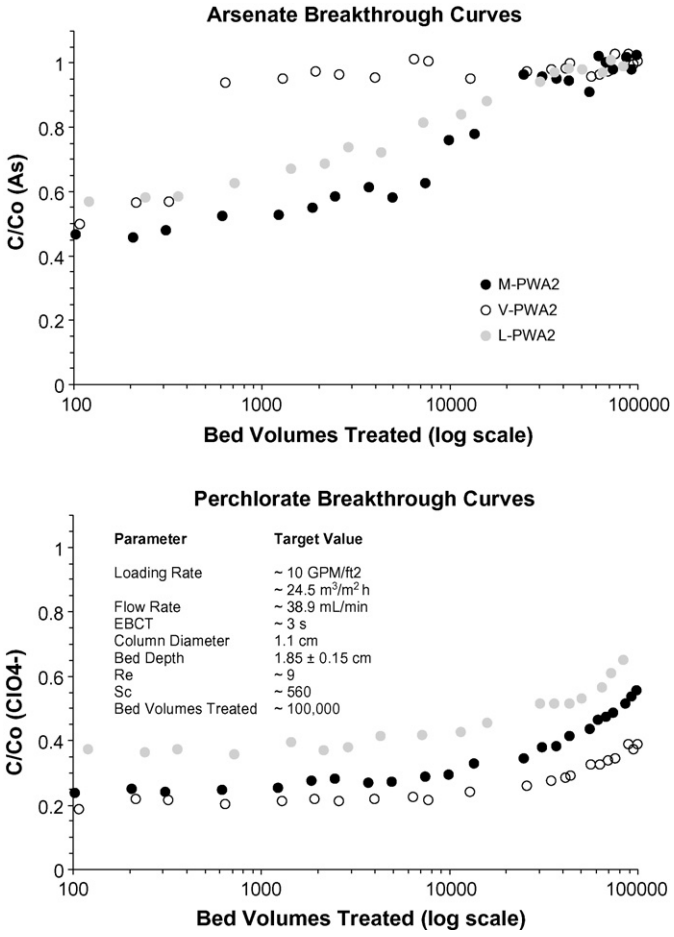

Fig. 6. Arsenic and perchlorate breakthrough curves for M-PWA2, L-PWA2 and V-PWA2 media in modified NSF53 Challenge water. $pH_{Effluent} \approx 7.6$; C_0 of As and $ClO_4^- \approx 100$ μg/L.

Gnielinski correlation [45]:

$$k_f = \frac{[1 + 1.5(1-\varepsilon)] \times D_l}{d_p} \times (2 + 0.644 \times Re^{1/2} \times Sc^{1/3}) \quad (7)$$

$$Re = \frac{\rho_l \times \Phi \times d_p \times v_l}{\varepsilon \times \mu_l} \quad (8)$$

$$Sc = \frac{\mu_l}{\rho_l \times D_l} \quad (9)$$

Constraints: $Re \times Sc > 500$; $0.6 < Sc < 10^4$; $1 < Re < 100$; $0.26 < \varepsilon < 0.935$.

Re is the Reynolds number (unitless), Sc the Schmidt number (unitless), d_p the adsorbent particle diameter ($d_p \approx 0.6 \times 10^{-3}$ m), D_l the free liquid diffusivity for arsenate or perchlorate, ε the bed void fraction ($\varepsilon \approx 0.45$), μ_l the dynamic viscosity of water at 20 °C (1.002×10^{-3} Ns/m^2), ρ_l the density of water at 20 °C ($\rho_l = 998.2$ kg/m^3), Φ the sphericity of the particle ($\Phi = 1$) and v_l is the liquid superficial velocity (m/s). The estimated the external mass transport coefficients were $k_{f(As)} \approx 6.1 \times 10^{-5}$ m/s and $k_{f(ClO_4^-)} \approx 9.8 \times 10^{-5}$ m/s, confirming the faster external mass transport of perchlorate.

The perchlorate breakthrough curve (Fig. 6) is characterized by a long, flat plateau that lasts for 5000–10,000 bed volumes

before effluent concentration slowly starts to increase. A plateau period is expected for a solute with minimal competitive adsorption by other solutes. The gradual breakthrough later in the run is also expected, as intraparticle mass transport (pore and/or surface diffusion) rather than external mass transport becomes the rate-limiting factor. The very small difference between the V-PWA2 and M-PWA2 breakthrough curves for perchlorate removal suggests that the perchlorate removal capacity of these two media is not very different, and that the removal capacity for perchlorate may not have to be greatly compromised to achieve necessary removal for both pollutants.

For the virgin media, effluent arsenate concentrations reach influent concentrations rapidly, within 1200 bed volumes, as Fig. 6 shows. In contrast, arsenic breakthrough takes substantially longer when HIX media is used. In all cases, HIX removed more arsenate than the virgin media. The shorter C/C_0 plateau and earlier breakthrough of arsenate compared to perchlorate may imply that competition by other solutes in the NSF 53 Challenge water (e.g., silica, phosphate) is affecting the adsorption of arsenate onto the iron (hydr)oxide in the media. As a result of the competition, the adsorption capacity for arsenate may be lower than the one estimated using batch tests where arsenate is sole adsorbate. Only small differences in the breakthrough curves of M-PWA2 and L-PWA2 were observed, which are related to minor variations in the experimental conditions, suggesting that the shape of the nanoparticles does not affect the overall transport of the media.

3.4. Issues related to development and use of IX media modified with nanostructured iron (hydr)oxide

One of the main concerns associated with development and use of nanomaterials in water treatment application is the risk of nanomaterial detachment and/or leaching into the treated effluent. Although the behavior of many metal (hydr)oxide nanoparticles in water environments and living organisms is not well understood, use of iron (hydr)oxide as arsenic treatment media has been well documented and rendered safe for use for many water treatment applications [46]. Even in a situation where iron (hydr)oxide nanomaterials from a media are leached into an effluent, the health risks could be considered nonexistent since iron (hydr)oxide is easily converted into soluble and non-harmful Fe^{3+} when exposed to an acidic environment (e.g., stomach acid).

In many cases, a treatment train system containing two columns in series may also be a viable option to remove arsenate and perchlorate. However, these types of systems may be cumbersome for applications where the size of the treatment system is an important factor such as small point-of-use treatment systems. Although the HIX media may be more expensive that traditionally used GFH and IX media, a smaller system containing HIX may be less expensive to operate and maintain.

4. Conclusion

The development and design of hybrid ion-exchange media containing nanoparticles should consider the impact of the nanoparticle impregnation process onto the ion-exchange performance of the media. Fabrication methods that can allow more even distribution of the nanoparticles throughout the media pores could contribute to a higher adsorption capacity and separation factor of the HIX media. Use of oxidizers during the fabrication process can decrease the separation factor of the media probably as a result of oxidation of the ion-exchange base material of the polymer. Ion-exchange media characterized with high porosity should be considered as a base material to reduce the possibility of pore clogging, which could additionally slow the intraparticle mass transport. Beyond HIX media for arsenate and perchlorate treatment, other HIX media could be also fabricated to simultaneously remove a large number of ions such as phosphates and nitrates that pose health or environmental risk.

Acknowledgements

This work was partially supported by the US EPA and Battelle Memorial Institute. Prof. John Crittenden for provided assistance. Thanks to Marisa Masles for the help with the IC, and Thomas Groy for the help with the XRD. Also thanks to Grant, Dewey and the Center for Solid State at Arizona State University.

References

[1] E.T. Urbanski, Perchlorate chemistry: implications for analysis and remediation, Bioremediation 2 (1998) 81–95.
[2] K. Christen, Perchlorate mystery surfaces in Texas, Environ. Sci. Technol. A 37 (21) (2003) 376(A)–377(A).
[3] P.K. Dasgupta, P.K. Martinelango, W.A. Jackson, T.A. Anderson, K. Tian, R.W. Tock, S. Rajagopalan, The origin of naturally occurring perchlorate: the role of atmospheric processes, Environ. Sci. Technol. 39 (6) (2005) 1569–1575.
[4] N.L. Plummer, J.K. Böhlke, M.W. Doughten, Perchlorate in pleistocene and holocene groundwater in north-central New Mexico, Environ. Sci. Technol. 40 (6) (2006) 1757–1763.
[5] C.E. Bradford, J. Rinchard, J.A. Carr, C. Theodorakis, Perchlorate affects thyroid function in Eastern Mosquitofish (*Gambusia holbrooki*) at environmentally relevant concentrations, Environ. Sci. Technol. 39 (14) (2005) 5159–5195.
[6] M. Tonnachera, A. Pinchera, A. Dimida, E. Ferrarini, P. Agretti, P. Vitti, F. Santini, K. Crump, J. Gibbs, Relative potencies and additivity of perchlorate, thiocyanate, nitrate, and iodide on the inhibition of radioactive iodide uptake by the human sodium iodide symporter, Thyroid 14 (2004) 1012–1019.
[7] US EPA, Perchlorate Treatment Technology Update, US EPA, Washington, DC, 2005 (EPA 542-R-05-015).
[8] US Department of Health and Human Services (Ed.), Toxicological Profile for Arsenic, US Department of Health and Human Services, Washington, DC, 2000.
[9] P.L. Smedley, D.G. Kinniburgh, A review of the source, behaviour and distribution of arsenic in natural waters, Appl. Geochem. 17 (5) (2002) 517–568.
[10] R.D. Foust, P. Mohapatra, A.M. Compton-O'Brien, J. Reifel, Groundwater arsenic in the Verde Valley in central Arizona, USA, Appl. Geochem. 19 (2) (2004) 251–255.
[11] R.J. Edmonds, D.J. Gellenbeck, Groundwater Quality in the West Salt River Valley, Arizona 1996-98—Relations to Hydrogeology, Water Use, and Land Use, Water Resources Investigation Report 01-4126, USGS, Tucson, Arizona, 2002.
[12] US EPA, Implementation Guidance for the Arsenic Rule, Office of Water, US EPA, Washington, DC, 2002 (EPA-816-K-02-018).

[13] EU Council, Council Directive 98/83/EC of 3 November 1998 on the quality of water intended for human consumption, Off. J. Eur. Communities L330 (1998) 32–54.
[14] WHO (Ed.), Guidelines for Drinking-Water Quality, World Health Organization, Geneva, 2004.
[15] N. Greenwood, A. Earnshaw, Chemistry of the Elements, Reed Educational and Professional Publishing Ltd., Woburn, MA, USA, 1997.
[16] B.H. Gu, Y.K. Ku, G.M. Brown, Sorption and desorption of perchlorate and U(VI) by strong-base anion-exchange resins, Environ. Sci. Technol. 39 (3) (2005) 901–907.
[17] A.R. Tripp, D.A. Clifford, Ion exchange for the remediation of perchlorate-contaminated drinking water, J. Am. Water Works Assoc. 98 (4) (2006) 105–114.
[18] G.A. Waychunas, B.A. Rea, C.C. Fuller, J.A. Davis, Surface-chemistry of ferrihydrite. 1: Exafs studies of the geometry of coprecipitated and adsorbed arsenate, Geochim. Cosmochim. Acta 57 (10) (1993) 2251–2269.
[19] D.M. Sherman, S.R. Randall, Surface complexation of arsenic(V) to iron(III) (hydr)oxides: structural mechanism from ab initio molecular geometries and EXAFS spectroscopy, Geochim. Cosmochim. Acta 67 (22) (2003) 4223–4230.
[20] V. Lenoble, O. Bouras, V. Deluchat, B. Serpaud, J.C. Bollinger, Arsenic adsorption onto pillared clays and iron oxides, J. Colloid Interface Sci. 255 (1) (2002) 52–58.
[21] M. Badruzzaman, P. Westerhoff, D.R.U. Knappe, Intraparticle diffusion and adsorption of arsenate onto granular ferric hydroxide (GFH), Water Res. 38 (18) (2004) 4002–4012.
[22] P. Westerhoff, D. Highfield, M. Badruzzaman, Y. Yoon, Rapid small-scale column tests for arsenate removal in iron oxide packed bed columns, J. Environ. Eng.-Asce 131 (2) (2005) 262–271.
[23] S. Bang, M. Patel, L. Lippincott, X.G. Meng, Removal of arsenic from groundwater by granular titanium dioxide adsorbent, Chemosphere 60 (3) (2005) 389–397.
[24] W. Zhang, P. Singh, E. Paling, S. Delides, Arsenic removal from contaminated water by natural iron ores, Miner. Eng. 17 (4) (2004) 517–524.
[25] R.P.S. Suri, J.B. Liu, J.C. Crittenden, D.W. Hand, Removal and destruction of organic contaminants in water using adsorption, steam regeneration, and photocatalytic oxidation: a pilot-scale study, J. Air Waste Manage. Assoc. 49 (8) (1999) 951–958.
[26] Z.M. Gu, J. Fang, B.L. Deng, Preparation and evaluation of GAC-based iron-containing adsorbents for arsenic removal, Environ. Sci. Technol. 39 (10) (2005) 3833–3843.
[27] M.J. DeMarco, A.K. Sengupta, J.E. Greenleaf, Arsenic removal using a polymeric/inorganic hybrid sorbent, Water Res. 37 (1) (2003) 164–176.
[28] A.I. Zouboulis, I.A. Katsoyiannis, Arsenic removal using iron oxide loaded alginate beads, Ind. Eng. Chem. Res. 41 (24) (2002) 6149–6155.
[29] F.S. Zhang, H. Itoh, Iron oxide-loaded slag for arsenic removal from aqueous system, Chemosphere 60 (3) (2005) 319–325.
[30] L. Cumbal, A.K. Sengupta, Arsenic removal using polymer-supported hydrated iron(III) oxide nanoparticles: role of Donnan membrane effect, Environ. Sci. Technol. 39 (17) (2005) 6508–6515.
[31] S.A. Crosby, D.R. Glasson, A.H. Cuttler, I. Butler, D.R. Turner, M. Whitfield, G.E. Millward, Surface areas and porosities of Fe(III)- and Fe(II)-derived oxyhydroxides, Environ. Sci. Technol. 17 (12) (1983) 709–713.
[32] A.K. Sengupta, L.H. Cumbal, Method of manufacture and use of hybrid anion exchanger for selective removal of contaminating fluids, US Patent Application 20,050,156,136, July 21 (2005).
[33] US EPA, SW-846 Test Methods for Evaluating Solid Waste, Physical/Chemical Methods, US EPA, Washington, DC, USA, 1996.
[34] J.C. Crittenden, R.R. Trussell, D.W. Hand, K.J. Howe, G. Tchobanoglous (Eds.), Water Treatment: Principles and Design, second ed., Wiley & Sons, Inc., Hoboken, New Jersey, USA, 2005.
[35] W.D. Schecher, D.C. McAvoy, D. William, MINEQL+ A Chemical Equilibrium Modeling System: Version 4. 0 for Windows User's Manual, Environmental Research Software, Hallowell, Maine, 1988.
[36] D.D. Endicott, W.J. Weber, Lumped-parameter modeling of multicomponent adsorption in the treatment of coal-conversion wastewater by GAC, Environ. Prog. 4 (2) (1985) 105–111.
[37] J.C. Crittenden, D.W. Hand, H. Arora, B.W. Lykins Jr., Design considerations for GAC treatment of organic chemicals, J. Am. Water Works Assoc. 79 (1) (1987) 74–82.
[38] W.J. Weber, E.H. Smith, Simulation and design models for adsorption processes, Environ. Sci. Technol. 21 (11) (1987) 1040–1050.
[39] M.C. Carter, W.J. Weber, Modeling adsorption of TCE by activated carbon preloaded by background organic matter, Environ. Sci. Technol. 28 (4) (1994) 614–623.
[40] D.R.U. Knappe, V.L. Snoeyink, P. Roche, M.J. Prados, M.M. Bourbigot, Atrazine removal by preloaded GAC, J. Am. Water Works Assoc. 91 (10) (1999) 97–109.
[41] M.A.H. Franson, A.D. Eaton, L.S. Clesceri, A.E. Greenberg (Eds.), Standard Methods for the Examination of Water and Wastewater, 19th ed., American Public Health Association, Washington, DC, USA, 1995.
[42] A. Sperlich, A. Werner, A. Genz, G. Amy, E. Worch, M. Jekel, Breakthrough behavior of granular ferric hydroxide(GFH) fixed-bed adsorption filters: modeling and experimental approaches, Water Res. 39 (2005) 1190–1198.
[43] E.H. Smith, W.J. Weber, Modeling activated carbon adsorption of target organic-compounds from leachate-contaminated groundwaters, Environ. Sci. Technol. 22 (3) (1988) 313–321.
[44] D. Lide (Ed.), CRC Handbook of Chemistry and Physics, 87th ed., Talor and Francis Group, Boca Raton, Florida, 2006.
[45] H. Sontheimer, J.C. Crittenden, S. Summers, Activated Carbon for Water Treatment, second ed., DVGW-Forschungsstelle, Engler-Bunte Institut, Universitat Karlsruhe, Karlsruhe, Germany, 1988.
[46] D. Mohan Jr, C.U. Pittman, Arsenic removal from water/wastewater using adsorbents—a critical review, J. Hazard. Mater. 142 (1–2) (2007) 1–53.